Synthetic Metals 162 (2012) 748–752

Contents lists available at SciVerse ScienceDirect

Synthetic Metals

journal homepage: www.elsevier.com/locate/synmet

Electronic properties of small molecule-diketopyrrolopyrrole derivatives and a correlation with the open circuit voltage in organic solar cells

Jung Hwa Seo*

Department of Materials Physics, College of Natural Science, Dong-A University, 840 Hadan2dong, Sahagu, Busan 604-714 Republic of Korea

ARTICLE INFO

Article history:
Received 16 November 2011
Received in revised form 20 February 2012
Accepted 24 February 2012

Keywords:
Organic solar cells
Ultraviolet photoelectron spectroscopy (UPS)
UV–vis absorption
Electronic structures
Open circuit voltage

ABSTRACT

The electronic properties of five diketopyrrolopyrrole (DPP) derivatives as a function of alkyl chains and conjugated frameworks were investigated. The results of ultraviolet photoelectron spectroscopy (UPS) and UV–vis absorption measurements show different ionization potentials (*IPs*), and optical band gaps. To investigate the relation between the *IP* and the open circuit voltage (V_{OC}) of bulk heterojunction (BHJ) solar cells, the V_{OC} of organic solar cells fabricated with DPP derivatives as the donor and [6,6]-phenyl C_{71} butyric acid methyl ester ($PC_{71}BM$) as the acceptor were measured. The values between the *IP* of the DPP derivatives and V_{OC} in BHJ devices exhibit linear relationship.

1. Introduction

Organic bulk heterojunction (BHJ) solar cells have been a subject of many recent investigations because the active layer can be deposited over large areas in a single step using low-cost fabrication techniques such as roll-to-roll coating, inkjet printing, and spin coating [1,2]. Recently, BHJ solar cells using a *p*-type polymer, thieno[3,4-b]thiophene and benzodithiophene polymers, as an electron donor and a soluble *n*-type fullerene, (6,6)-phenyl C_{71} butyric acid methylester ($PC_{71}BM$), as an electron acceptor have achieved power conversion efficiency (*PCE*) up to ~7% [3]. The *PCE* of organic solar cells depends on the short circuit current density (J_{SC}), the open circuit voltage (V_{OC}), and the fill factor (*FF*), $PCE = (J_{SC}V_{OC}FF)/P_0$, where P_0 is the incident light intensity [4,5]. In BHJ solar cells, there has been a general acceptance that V_{OC} depends on the energy difference between the ionization potential (*IP*) of the electron donor material and the electron affinity (*EA*) of the electron acceptor material [6]. Recently, a series of poly(thiophene) derivatives were synthesized and their oxidation potentials were correlated to V_{OC} of BHJ solar cells using a fullerene derivative as the acceptor [7]. From materials design, the *PCE* of many reported BHJ solar cells is limited by the low V_{OC} (~0.6 V), a result of having a smaller highest occupied molecular orbital (HOMO) or *IP*, and the narrow energy gap of donor materials (~2 eV) [8]. It is therefore critical to enhance V_{OC}, while maintaining the corresponding J_{SC} and *FF*. One method to improve V_{OC} is to design materials having a larger or deeper *IP* [9,10]. To reduce the band gap, a common approach is to incorporate strong electron-donating and electron-accepting moieties within a conjugated backbone [11].

In search for new donor materials with easy synthesis, purification, and functionalization, one can find diketopyrrolopyrrole (DPP)-based materials exhibiting bright and strongly fluorescent with exceptional photochemical, mechanical, and thermal stability [12–17]. These materials have been used in industrial applications as high performance pigments in paints, plastics and inks. Combining DPP core with thiophene, phenylene and benzofuran building blocks and appropriate functional groups leads to materials that have tunable band gap, energy levels, and molecular packing that can be used in BHJ solar cells and thin film transistors [13,18–22].

Cyclic voltammetry (CV) is a common method for determining the HOMO and the lowest unoccupied molecular orbital (LUMO) levels of organic compounds [23]. However, this information is obtained in solution and in the presence of an electrolyte. As previous reports have shown, the situation in neat film is different [24,25]. For this reason, ultraviolet photoelectron spectroscopy (UPS) should be used to study energy levels of solar cell materials. UPS is a well-established analytical technique for studying energy levels in organic thin films. When UV photons are incident on the sample, electrons from occupied states are ejected to the vacuum. The kinetic energies of the escaping electrons are measured, revealing information about the interfacial electronic structures such as the HOMO levels, work function, *IP* and interfacial dipole [26,27].

In this work, five new low band gap DPP-based materials were synthesized for use as donors in solution-processable BHJ solar

* Tel.: +82 51 200 7233; fax: +82 51 200 7232.
E-mail address: seojh@dau.ac.kr

0379-6779/$ – see front matter © 2012 Elsevier B.V. All rights reserved.
doi:10.1016/j.synthmet.2012.02.026

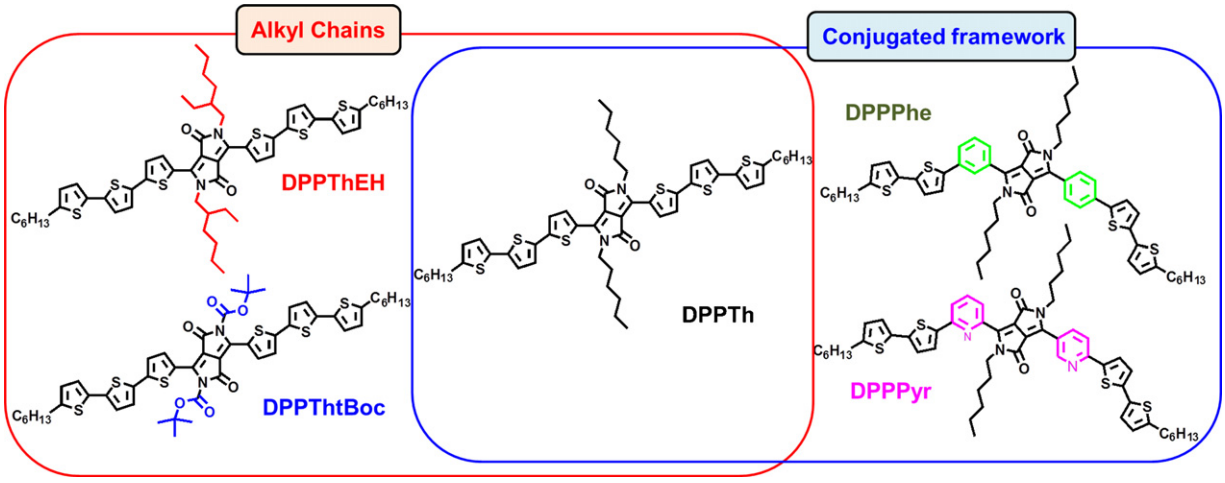

Fig. 1. Chemical structures of DPP derivatives.

cells (Fig. 1). The materials are divided into two groups: DPPThEH, DPPThtBoc, DPPTh and DPPTh, DPPPhe, DPPPyr where the substituting alkyl chains and the conjugated units attached to the DPP core are varied, respectively. Then influences in the optical band gap, energy levels, thin film morphology, and V_{OC} as altering chemical structures were examined using absorption spectroscopy, UPS, atomic force microscopy (AFM), and solar cell devices, respectively. Solution-processed BHJ solar cells using the five materials as donors and $PC_{71}BM$ as an acceptor were fabricated to correlate between the electronic structures and the device characteristics.

2. Experimental

Detailed synthetic methods for DPP derivatives are described in the literature [13,18,20–22]. Solutions were prepared in chloroform and handled in a nitrogen filled glovebox. UV–vis absorption measurements were performed on a Beckman Coulter DU 800 Spectrophotometer and films were spin-coated from 0.6% (w/v) solutions onto quartz substrates. For UPS experiments, an 80 nm-thick Au film was deposited on a precleaned Si substrate with a thin native oxide (Angstrom Engineering). Subsequently, 0.1% (w/v) solution of each DPP derivative was spin-coated at 3000 rpm for 60 s atop the Au-coated Si substrate. The thicknesses of the DPP derivatives were determined to be 2.8 nm for DPPThEH, 2.7 nm for DPPThtBoc, 3.6 nm for DPPTh, 4.0 nm for DPPPhe, and 4.4 nm for DPPPyr by AFM measurements. All film preparation was done in a N_2-atmosphere glovebox. To minimize possible influence by exposure to air, the films were then transferred from the glovebox to the UPS analysis chamber inside an air-tight sample holder. All samples were kept inside a high-vacuum chamber overnight to remove solvent residue. The UPS analysis chamber was equipped with a hemispherical electron energy analyzer (Kratos Ultra Spectrometer) and a UV (He I) source, and was maintained at 1×10^{-9} Torr. A sample bias of −9 V was used to acquire the high binding energy cutoff. To confirm reproducibility of UPS spectra, these measurements were repeated twice on two sets of samples.

The surface topographic images were obtained under ambient conditions using a Nanoscope IIIa/Multimode Scanning Probe Microscope (Veeco). All AFM images were obtained in tapping mode using Si probes having a resonant frequency of ~75 kHz and a spring constant of 1–5 N/m (Budget Sensors).

Organic solar cells were prepared according to the following procedure. Blended films of DPP and $PC_{71}BM$ (1:1 ratio) were spin coated at 900 rpm for 30 s from chloroform solutions (10 mg/mL) onto a 40 nm layer of poly(3,4–ethylenedioxythiophene):polystyrene sulfonate, PEDOT:PSS (H.C. Starck) onto indium tin oxide ITO-coated glass substrates. The active layer thicknesses of all devices obtained by using Ambios XP-100 profilometer were approximately 65 nm. Aluminum (500 Å) electrodes were thermally evaporated at a pressure of 1×10^{-7} Torr at room temperature using a shadow mask. Solar cells were characterized under simulated 100 mW/cm^2 AM1.5G irradiation from a Xe arc lamp with an AM1.5 global filter. All device fabrication and testing were conducted inside a nitrogen filled glovebox.

3. Results and discussions

Fig. 2 shows UV–vis absorption spectra of five DPP derivative films and all the relevant data are summarized in Table 1. All DPP derivatives exhibit remarkably different absorption characteristics depending on the nature of the side chains and substituted core structures. The absorption spectra show intense bands in both the ultraviolet and visible parts of the spectrum from 300 nm to 500 nm and from 500 nm up to 900 nm, respectively, with latter absorption feature being assigned to the DPP chromophore unit. The absorption band ~725 nm in the DPPThEH, DPPThtBoc, and DPPTh film has been observed previously in highly ordered oligothiophene-DPP systems and assigned to strong intermolecular interactions [13,18]. For the DPPTh, the first absorption peak of DPP band occurs at 568 nm, 87 nm blue-shifted compared to those of the DPPThEH

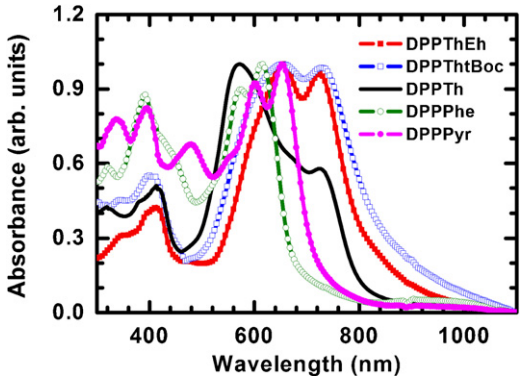

Fig. 2. UV–vis absorption spectra of DPPThEH, DPPThtBoc, DPPTh, DPPPhe, and DPPPyr thin films.

Table 1
Summary of electronic properties of all compounds studied here and their device parameters.

	$\lambda_{max}{}^1$ (nm)	$\lambda_{max}{}^2$ (nm)	λ_{onset} (nm)	E_g (eV)	IP (eV)	EA (eV)	J_{sc} (mA/cm^2)	V_{oc} (V)	FF (%)	PCE (%)
DPPThEH	655	724	844	1.47	4.92	3.45	9.2	0.75	44	3.0[a]
DPPThtBoc	656	729	868	1.43	4.86	3.43	5.4	0.65	34	1.2[b]
DPPTh	568	724	809	1.53	4.61	3.08	4.2	0.47	40	0.79
DPPPhe	574	615	680	1.82	5.11	3.29	4.5	0.87	37	1.45
DPPPyr	602	654	724	1.71	5.30	3.59	2.7	0.50	41	0.55

[a] Ref. [22].
[b] Ref. [20].

and DPPThtBoc films. The side chains of DPPEH and DPPtBoc are solvated more favorably by the solvent molecules than that of DPPTh. This can make the DPP derivatives with EH and tBoc side chains exhibit more expanded structures in the films resulted in a red-shift in the absorption spectrum. [28,29]. In addition, higher structural organization in DPPThEH and DPPThtBoc becomes more favorable as they have more expanded structures due to the different alkyl side chains [13,30].

Interestingly, change of the DPP core results in remarkably dissimilar absorption features. Replacing the thiophene units attached to the DPP core with phenyl rings (DPPPhe) and pyridines (DPPPyr) results in an intense absorption in the 300–500 nm regions and a much narrower and blue-shifted absorption band at ~600 nm. The corresponding optical energy gaps (E_g) estimated from the spectrum low-absorption band edge are ~1.47 eV for DPPThEH, ~1.43 eV for DPPThtBoc, 1.53 eV for DPPTh, 1.82 eV for DPPPhe, and 1.71 eV for DPPPyr, respectively. As expected, the E_g values for the DPPThEH, DPPThtBoc and DPPTh with different alkyl chains are similar since they have the same conjugated backbone. However, for DPPPhe and DPPPyr, modification of conjugated aryl groups next to the DPP core results in a slight increase in the E_g.

UPS spectra for DPPThEH, DPPThtBoc, DPPTh, DPPPhe, and DPPPyr thin films on Au-coated silicon substrates are shown in Fig. 3. The Fermi energy (E_F) was determined from the Au surface and all other spectra are plotted with respect to this value. In other words, the abscissa is the binding energy relative to the E_F of Au. The vacuum levels (VLs) of the samples were determined by linear extrapolation of secondary electron cutoffs (E_{SE}) on the high binding energy side of the UPS spectra (14–19 eV). Here the spectra have been shifted in the intensity direction to identify the lowest energy level. Deposition of the DPPThEH, DPPThtBoc, DPPTh, and DPPPhe leads to a shift of VLs toward higher energies, while for the DPPPyr the change is less pronounced. Fig. 3(b) shows the HOMO onsets for the five DPP derivatives. The HOMO energy levels of the DPP derivatives were calculated using the low binding energy region (0–3 eV). Comparing the shift in the HOMO onset (E_{HOMO}) in each film to the E_F of Au provides the relative position of the HOMO level. The E_{HOMO} of DPPThEH, DPPThtBoc, DPPTh, DPPPhe, and DPPPyr are (in eV) 0.56, 0.38, 0.26, 0.72, and 0.85, respectively. The IP is determined by using the incident photon energy (21.2 eV), the E_{SE},

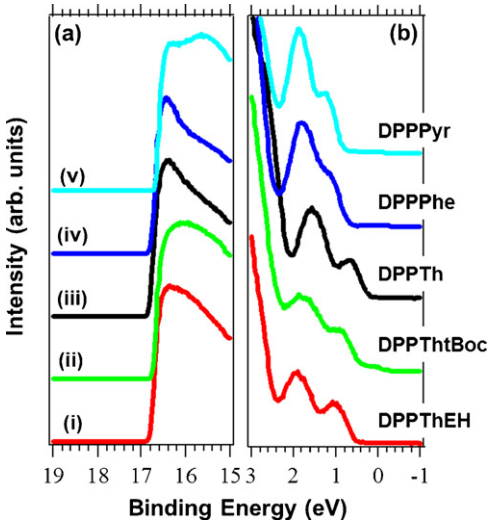

Fig. 3. UPS spectra of (a) the high binding energy cutoff region and (b) the HOMO region of (i) DPPThEH, (ii) DPPThtBoc, (iii) DPPTh, (iv) DPPPhe, and (iv) DPPPyr.

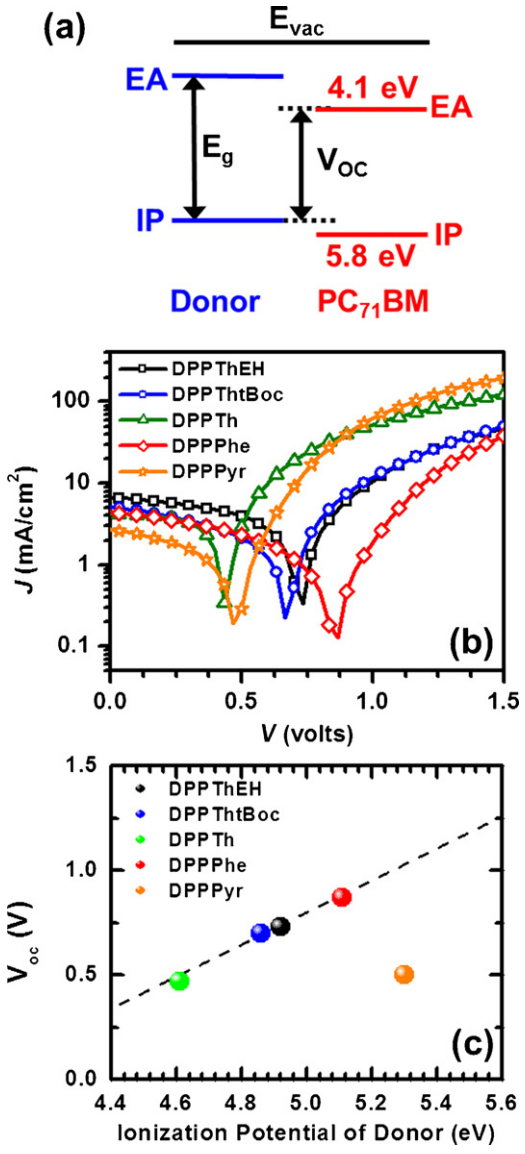

Fig. 4. (a) A schematic energy level diagram of a donor/$PC_{71}BM$ system, (b) J–V characteristics of the DPP derivatives:$PC_{71}BM$ bulk heterojunction (BHJ) solar cells. (c) The open-circuit voltage (V_{OC}) of BHJ cells plotted versus the ionization potential of the DPP derivatives as donor materials used in each individual device.

Table 2
Determination of the IP of small molecule-diketopyrrolopyrrole derivatives as a function of film thickness.

	DPPThEH		DPPThtBoc		DPPTh		DPPPhe		DPPPyr	
	Thin	Thick	Thin	Thick	Thin	Thick	Thin	Thick	Thin	Thick
Thickness (nm)	2.6	17.4	2.2	16.2	2.9	25.1	3.1	19.6	3.6	14.1
IP, HOMO (eV)	4.92	4.95	4.82	4.89	4.59	4.64	5.10	5.18	5.35	5.27
	4.93	4.87	4.83	4.88	4.58	4.62	5.10	5.05	5.33	5.23
Average IP (eV)	4.92 ± 0.03		4.86 ± 0.03		4.61 ± 0.02		5.11 ± 0.05		5.30 ± 0.05	

and the E_{HOMO} according to the equation, $IP = 21.2 - (E_{SE} - E_{HOMO})$ [24]. The *IPs* for DPPTh, DPPThtBoc, DPPThEH, DPPPhe, and DPPPyr are 4.6, 4.8, 4.9, 5.1, and 5.3 eV, and the results are summarized in Table 2 (the UPS spectra of thick films were not shown here).

One possible explanation about why the *IP* of the DPPThEH is lower than that of DPPTh (having the linear chain) are caused by different packing motifs. With the straight alkyl chain, the molecules can pack close to each other, while the branch alkyl chain, this packing is disrupted, resulting in electron decoupling and lowering the binding energy. This packing effect leads to fundamentally different electronic properties in solid states [31–33]. The detail information of the steric effect in all compounds is still under investigation.

A schematic energy diagram of a donor $PC_{71}BM$ system with the frontier energy levels and the V_{OC} is shown in Fig. 4(a). For these estimates an *EA* energy, −4.1 eV was used, which is on the high end of the values provided in the literature (−3.7 to −4.3 eV) and anticipated to yield a smaller V_{OC} [34]. Previous studies on conjugated polymer BHJ cells have shown that the difference between the donor *IP* and the acceptor *EA* limits the V_{OC}. The *EAs* of the DPP derivatives must be positioned above that of the $PC_{71}BM$ acceptor by at least about 0.3 eV to provide a driving force for efficient electron transfer from the donor to the acceptor (charge separation) [10,11]. Therefore, the ideal *EA* of DPP derivatives should be between 3.5 eV and 3.8 eV. For the donor material, the ideal E_g should range between 1.2 and 1.9 eV as more photons are present in the near IR region [6,8]. Therefore, the ideal *IP* should range between 5.0 and 5.4 eV which assures a high V_{OC} in BHJ solar cells. From the UPS results, the three DPP derivatives having the same backbone but different alkyl chains (DPPThEH, DPPThtBoc and DPPTh) show *IP* values at 4.6–4.9 eV. In contrast, DPPPhe and DPPPyr show different values of the *IPs* at 5.1–5.3 eV. For DPPTh, one can see a remarkable decrease of the *IP* when compared to the other DPP derivatives. Thus, substituting the thiophene units attached to the DPP core with phenyl or pyridine units induces a

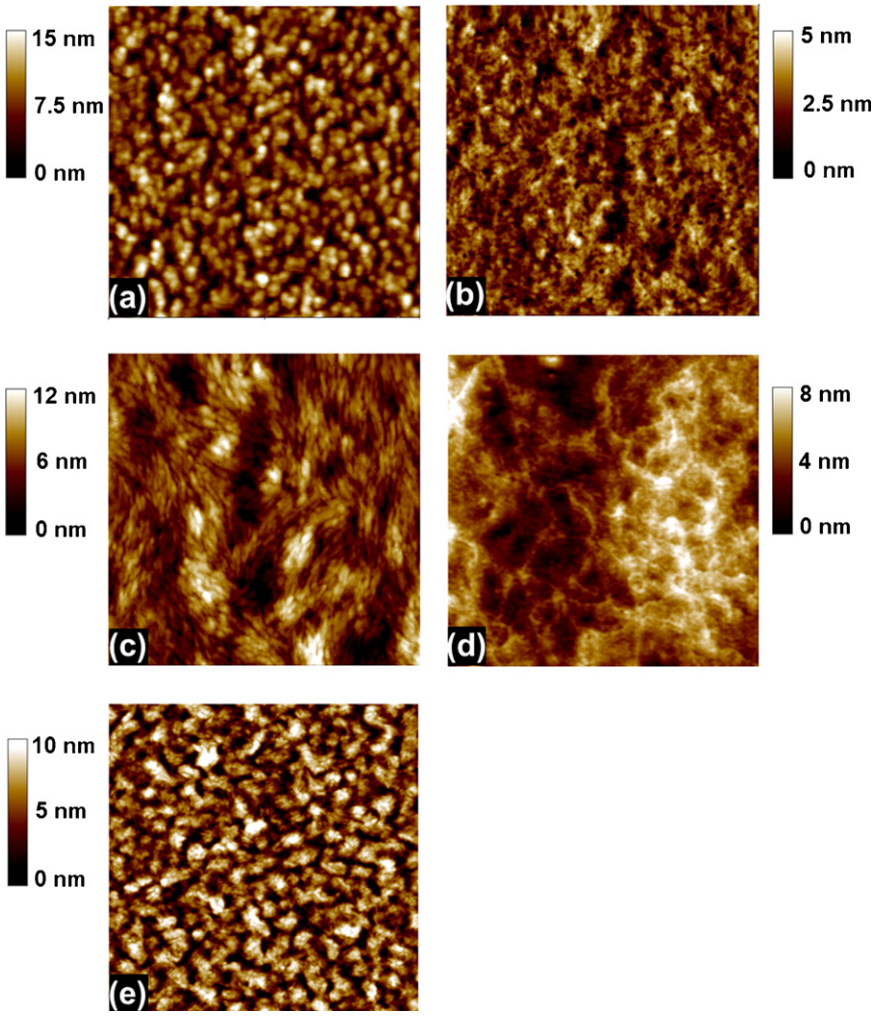

Fig. 5. AFM images (2 μm × 2 μm) of (a) DPPThEH, (b) DPPThtBoc, (c) DPPTh, (d) DPPPhe, and (e) DPPPyr with $PC_{71}BM$ blended on PEDOT:PSS/ITO substrates.

clear increase of *IP* and should result in a higher V_{OC}. This is mainly due to relatively lower electron donating ability of both phenyl and pyridyl ring than a thienyl ring.

To support our predictions and demonstrate the potential of DPP derivatives as an electron donor in organic solar cells, these new DPP derivatives were tested in BHJ solar cells with $PC_{71}BM$ as an acceptor. The current density versus voltage (*J–V*) characteristics of solar cells with the five DPP derivatives:$PC_{71}BM$ composites are shown in Fig. 4(b) and device parameters were summarized in Table 1. The highest V_{OC} (0.87 eV) is obtained from DPPPhe:$PC_{71}BM$ device, while the lowest V_{OC} (0.47 eV) is obtained from the DPPTh:$PC_{71}BM$ cell.

In Fig. 4(c), the V_{OC} values of DPP derivatives:$PC_{71}BM$ solar cells are plotted against the *IPs* of the five DPP derivatives used as a donor in these devices. A good linear fit through the data indicates a good correlation of the *IP* determined from UPS and the V_{OC} of DPP derivatives:$PC_{71}BM$ BHJ solar cells. Among the five compounds, the DPPPyr:$PC_{71}BM$ device has much lower V_{OC} than the expected trend. Perhaps, factors other than the difference between the energy levels of the donor *IP* and the acceptor *EA* may influence the device V_{OC}. The dependence of V_{OC} on the illumination intensity and temperature as well as the strength of the donor intermolecular interactions has been shown for small molecule-based solar cells [35–37].

Since it is known that the morphology of the active material in BHJ solar cells significantly affects the device performance [38–40], DPP derivatives:$PC_{71}BM$ surface morphology was investigated by tapping mode AFM as shown in Fig. 5. The root mean square (rms) roughness of DPPThEH, DPPThtBoc, DPPTh, DPPPhe, and DPPPyr are (in nm) 2.21, 0.62, 1.62, 0.88, and 5.23, respectively. The DPPThtBoc:$PC_{71}BM$ film surface is very smooth, while the DPPPyr:$PC_{71}BM$ film surface is a significantly rough. Perhaps, the mismatch of between the *IP* and the V_{OC} of DPPPyr shown in Fig. 4(c) can be explained that the V_{OC} is also affected in certain degree by the morphology of the blend. Nevertheless, the energy levels of DPP derivatives provide a good estimation of the V_{OC} considering a similar tendency with variations of the *IP*. Based on these data, modification of chemical structures can thus be used to control the *IP* and the *EA* of materials as well as V_{OC} in BHJ solar cells.

4. Conclusions

The five DPP derivatives as a function of alkyl chains and conjugated aryl groups around the DPP core were studied. The results of UPS and UV–vis absorption measurements show different molecular orbital levels, the *IP*, and optical band gaps. To understand the relation between the *IP* and the V_{OC} of BHJ solar cells, DPP derivative:$PC_{71}BM$ blend cells were fabricated. The *IP* and the V_{OC} exhibit linear relation and the values of V_{OC} obtained from BHJ solar cells, consistent with the energy difference between the *IP* of the DPP derivatives and the *EA* of $PC_{71}BM$ layer. Taking all these data into account, one can conclude that DPPPhe has the best potential for photovoltaic devices. It is anticipated that these values obtained from BHJ solar cells could be improved through modification in the device fabrication (solvent, different ration of blend solutions, film thickness, annealing, etc.). Based on the findings presented in this work, control of V_{OC} can be realized together with the enhancement in device performance of BHJ solar cells. These studies are thus important for understanding how these materials function in organic solar cells, contributing to the improvement of device performance and the design of new materials for use in organic solar cells.

Acknowledgment

The author thanks Prof. T.-Q. Nguyen and Dr. A. B. Tamayo for experimental supports and materials. This work was supported by the Dong-A University research fund.

References

[1] N.S. Sariciftci, L. Smilowitz, A.J. Heeger, F. Wudl, Science 258 (1992) 1474.
[2] R.C. Coffin, J. Peet, J. Rogers, G.C. Bazan, Nat. Chem. 1 (2009) 657.
[3] Y. Liang, Z. Xu, J. Xia, S.-T. Tsai, Y. Wu, G. Li, C. Ray, L. Yu, Adv. Mater. 22 (2010) E135.
[4] Y. Kim, S. Cook, S.M. Tuladhar, S.A. Choulis, J. Nelson, J.R. Durrant, D.D.C. Bradley, M. Giles, I. McCulloch, C.-S. Ha, M. Ree, Nat. Mater. 5 (2006) 197.
[5] P.W. Blom, V.D. Mihailetchi, L.J.A. Koster, D.E. Markov, Adv. Mater. 19 (2007) 1551.
[6] M.C. Scharber, D. Mühlbacher, M. Koppe, P. Denk, C. Waldauf, A.J. Heeger, C.J. Brabec, Adv. Mater. 18 (2006) 789.
[7] A. Gadisa, M. Svensson, M.R. Andersson, O. Inganäs, Appl. Phys. Lett. 84 (2004) 1609.
[8] G. Dennler, M.C. Scharber, C.J. Brabec, Adv. Mater. 21 (2009) 1323.
[9] J.C. Bijleveld, M. Schahid, J. Gilot, M.M. Wienk, R.A.J. Janssen, Adv. Funct. Mater. 19 (2009) 3262.
[10] N. Blouin, A. Michaud, D. Gendron, S. Wakim, E. Blair, R. Neagu-Plesu, M. Belletête, G. Durocher, Y. Tao, M. Leclerc, J. Am. Chem. Soc. 130 (2008) 732.
[11] S.H. Park, A. Roy, S. Beaupré, S. Cho, N. Coates, J.S. Moon, D. Moses, M. Leclerc, K. Lee, A.J. Heeger, Nat. Photonics 3 (2009) 297.
[12] Z. Hao, A. Iqbal, Chem. Soc. Rev. 26 (1997) 203.
[13] P. Sonar, G.-M. Ng, T.T. Lin, A. Dodabalapur, Z.-K. Chen, J. Mater. Chem. 20 (2010) 3626.
[14] K.A. Mazzio, M. Yuan, K. Okamoto, C.K. Luscombe, ACS Appl. Mater. Inter. 3 (2011) 271.
[15] B. Walker, A.B. Tamayo, X.-D. Dang, P. Zalar, J.H. Seo, A. Garcia, M. Tantiwiwat, T.-Q. Nguyen, Adv. Func. Mater. 19 (2009) 3063.
[16] F. Saremi, G. Lange, B. Tieke, Adv. Mater. 8 (1996) 923.
[17] B. Song, S. Wang, X. Zhang, Y. Fu, M. Smet, W. Dehaen, Angew. Chem., Int. Ed. 44 (2005) 4731.
[18] M. Tantiwiwat, A.B. Tamayo, N. Luu, X.-D. Dang, T.-Q. Nguyen, J. Phys. Chem. C 112 (2008) 17402.
[19] D. Cao, Q. Liu, W. Zeng, S. Han, J. Peng, S. Liu, J. Polym. Sci. Part A 44 (2006) 2395.
[20] A.B. Tamayo, M. Tantiwiwat, B. Walker, T.-Q. Nguyen, J. Phys. Chem. C 112 (2008) 15543.
[21] A.B. Tamayo, B. Walker, T.-Q. Nguyen, J. Phys. Chem. C 112 (2008) 11545.
[22] A.B. Tamayo, X.-D. Dang, B. Walker, J. Seo, T. Kent, T.-Q. Nguyen, Appl. Phys. Lett. 94 (2009) 103301.
[23] M.N. Chaur, F. Melin, B. Elliott, A.J. Athans, K. Walker, B.C. Holloway, L. Echegoyen, J. Am. Chem. Soc. 129 (2007) 14826.
[24] J.H. Seo, T.-Q. Nguyen, J. Am. Chem. Soc. 130 (2008) 10042.
[25] B.W. D'Andrade, S. Datta, S.R. Forrest, P. Djurovich, E. Polikarpov, M.E. Thompson, Org. Electron. 6 (2005) 11.
[26] Y. Gao, Acc. Chem. Res. 32 (1999) 247.
[27] J. Hwang, E.-G. Kim, J. Liu, J.-L. Brèdas, A. Duggal, A. Kahn, A. J. Phys. Chem. C 111 (2007) 1378.
[28] J. Cornil, I. Gueli, A. Dkhissi, J.C. Sancho-Garcia, E. Hennebicq, J.P. Calbert, V. Lemaur, D. Beljonne, J.L. Brédas, J. Chem. Phys. 118 (2003) 6815.
[29] R.D. McCullough, S. Tristram-Nagle, S.P. Williams, J. Am. Chem. Soc. 115 (1993) 4910.
[30] R.L. Elsenbaumer, K.-Y. Jen, R. Oboodi, Synth. Met. 15 (1986) 169.
[31] S. Duhm, H. Glowatzki, J.P. Rabe, N. Koch, R.L. Johnson, Appl. Phys. Lett. 88 (2006) 203109.
[32] F. Garnier, A. Yassar, R. Hajlaoui, G. Horowitz, F. Deloffre, B. Servet, S. Ries, P. Alnot, J. Am. Chem. Soc. 115 (1993) 8716.
[33] R. Friedlein, X. Crispin, C. Suess, M. Pickholz, W.R. Salaneck, J. Chem. Phys. 121 (2004) 2239.
[34] M.O. Reese, M.S. White, G. Rumbles, D.S. Ginley, S.E. Shaheen, Appl. Phys. Lett. 92 (2008) 053307.
[35] P. Kumar, S.C. Jain, H. Kumar, S. Chand, V. Kumar, Appl. Phys. Lett. 94 (2009) 183505.
[36] M.D. Perez, C. Borek, S.R. Forrest, M.E. Thompson, J. Am. Chem. Soc. 131 (2009) 9281.
[37] S. Uchida, J. Xue, B.P. Rand, S.R. Forrest, Appl. Phys. Lett. 84 (2004) 4218.
[38] L. Liu, Y. Shi, Y. Yang, Adv. Funct. Mater. 11 (2001) 420.
[39] H. Hoppe, N.S. Sariciftci, J. Mater. Chem. 16 (2006) 45.
[40] J.K.J. Duren, X. Yang, J. Loos, C.W.T. Bulle-Lieuwma, A.B. Sieval, J.C. Hummelen, R.A.J. Janssen, Adv. Funct. Mater. 14 (2004) 425.